LIP-VIREO in Action

Version 1.26

Author: Wan-Lei Zhao

Date: 26-Jan-2012

Preface

Image local features (also known as keypoint features) have been widely explored in the last decade due to its unique advantages over image global features. They have been successfully applied in wide range of applications and systems, such as wide baseline matching, object retrieval and recognition, and near-duplicate image/video detection. Comparing with global features, image local feature characterizes image at a more fine-grained level. Due to the success of the keypoint detectors (e.g., Harris and DoG) and descriptors (e.g., SIFT and SURF), these tasks are no longer as challenging as they were thought many years ago. Tasks such as visual object detection and recognition become also tractable. Although there are already many contexts the keypoint feature can fit in, it seems still too early to say we have witnessed how best the keypoint feature might actually bring us.

The development of this toolkit is a reflection of stat-of-the-art research on keypoint features. Since as indicated in many research works, it is hard to find any detector or descriptor performs the best all the time, allowing user to choose among as many as possible options is desirable. Such that user may explore and try them with different combinations under different contexts. So it would not be surprising some new properties will be discovered from long existing features some day. Bear this in mind, I try to cover popular detectors and descriptors as much as possible in the toolkit. However, I might not be able to catch up the recent progress in the literature due to the limited spare time, limited resources and most of all, fast growing of this area. To this point, beg your tolerance and patience!

The development of this toolkit is out of the personal interests. I am not regretful that hundreds of weekends were spent on this interesting topic. Instead, it is my pleasure that finally it turns out to be helpful to others as it grows reasonably big. Wish it could be more stable and powerful as time goes on. However, for the limited time I can spend on it, it is not promised to fix the known bugs timely and work out a new release regularly. However any bug reports or suggestions are appreciated all the time.

In this manual, the basic theories and the implementation of each detector and descriptor are reviewed briefly. We try to outline the brief idea behind each detector and descriptor. This helps user to understand how they work and what the potential drawbacks they might have. User is also provided with the basic hints based on which one is able to choose the suitable combination (between detector and descriptor) for his specific task. In order to avoid possible confusion about our implementation and original versions from the author, the differences that our implementation from original paper are highlighted. For the user who wants to repeat the implementation, referring

to the original papers or implementations is encouraged.

In addition, a brief evaluation on the performances of the detectors and descriptors are presented in the end of corresponding chapters. The evaluations are conducted on popular datasets, which makes it easier to objectively judge the performances of different detectors and descriptors. However, the evaluation might only reflect the behaviors of the detectors and descriptors of certain aspects, it is therefore not surprising that the performance rank changes when they are tested under other situations. The third part of this book is a manual to guide user how to work with **LIP-VIREO** comfortably. It includes the instructions on how to detect keypoints, how to extract the descriptors and how to visualize the detected keypoints.

Currently, **LIP-VIREO** supports keypoint feature extraction of various types. The detectors it covers are: *Harris-Laplacian* [1], *Hessian* [1], *Hessian-Laplacian* [1], *DoG* [2], *LoG* [7] , *Fast Hessian* [12] and *Dense sampling*. For each detector, one can choose to either output keypoints or display them in the image or both. The following keypoint descriptors have been integrated in LIP-VIREO. They are *SIFT* [2], *Flip invriant SIFT*, which is newly proposed by us, *PCA-SIFT* [3], *SURF* [12], *AoD*, SPIN image [6], RIFT [6] and Enhanced RIFT, FIND [18] and Steerable Filters which is also known as '*Local Jet*'. After several rounds of re-factoring, the framework and output format of **LIP-VIREO** become stabilized. For the sake of compatibility, new version is kept to behavior as it used to be as much as possible. However, major update could happen for good reason. For each new version, the release tries to cover all popular systems such as Windows, Linux, MacOS and Unix.

LIP-VIREO is partially implemented and fully maintained by me. The implementation of PCA-SIFT is fully from Dr. Ke Yan.

Contents

Chapter 1

Detectors

Currently, seven most popular detectors are integrated in **LIP-VIREO**. Namely, they are Harris-Laplacian, Hessian-Laplacian, Hessian, Fast Hessian (SURF detector), Difference of Gaussian (DoG), Laplacian of Gaussian (LoG) and Dense. In this chapter, fundamental theories and techniques about detectors are reviewed. In addition, a brief introduction about our implementations are given. Although we try to stick to the descriptions in the original papers, possible changes have made due to several reasons. In this case, we will point out the differences between our implementation and the original one. In the last section, a brief evaluation is conducted on the dataset provided by INRIA-LEAR [4]. Different image transformations such as scale, rotation, viewpoint changes have been considered. This evaluation acts as a reference for user. We don't verdict that the performance rank will be kept the same across various circumstances. The exploration on different combinations between detector and descriptors in different applications is left to the user. The instructions on how to choose among different detectors in the command line can be found in Section 3.1.

1.1 Harris and Harris-Laplacian Detectors

For approaches which are based on the saliency functions, different functions are adopted to measure the saliency of the region around a pixel. Harris [1] detector is mainly based on the second moment matrix which is defined in Eqn. 1.1 for a point X.

$$\mu(X, \sigma_I, \sigma_D) = \sigma_D^2 g(\sigma_I) * \begin{bmatrix} L_x^2(X, \sigma_D) & L_x L_y(X, \sigma_D) \\ L_x L_y(X, \sigma_D) & L_y^2(X, \sigma_D) \end{bmatrix}, \tag{1.1}$$

where σ_I is the integration scale, σ_D is the differentiation scale and L_g is the derivative computed in the g (x or y) direction. This matrix mainly describes the gradient distribution in a local neighborhood of point X. The local derivatives are computed with Gaussian kernels of the size determined by the local scale σ_D (differentiation scale). The derivatives are then averaged in the neighborhood of the points by smoothing with a Gaussian window of size σ_I (integration scale). The eigenvalues of this matrix represent two principal signal changes in the neighborhood of a point. Based on this function, Harris detector favors pixels which hold large curvature values in both principal directions.

The selection function is therefore defined as Eqn. 1.2.

$$Harris(X, \sigma_I, \sigma_D) = |\mu(X, \sigma_I, \sigma_D)| - \alpha * trace^2(\mu(X, \sigma_I, \sigma_D)), \tag{1.2}$$

where α is a constant. Consequently, local interest point is identified at where one pixel attains local maxima with respect to *cornerness*. The local maxima can be identified after non-maximal suppression.

In order to achieve scale invariance, an appropriate scale must be chosen for each detected local interest point. This process involves in seeking local extrema in the scale space. In the scale-adapted second moment matrix (Eqn. 1.1), parameter σ_I determines the scale of local region centering on point X. Different σ_I result in different local maxima of function 1.2. However, not all the local maximas generated by different σ_I are meaningful. According to [7], only local maximas which achieve local extrema in scale space turn out to be stable and coincide with local structures well. Furthermore, σ_D is still an unknown variable. To simplify the problem, σ_D is related to σ_I by a constant ratio, e.g., $\sigma_D = 0.8 \cdot \sigma_I$. As a result, the problem of seeking proper parameters σ_I and σ_D has been reduced to searching for local extrema in the scale space.

However, as indicated by T. Lindeberg [7], Eqn. 1.2 rarely attains maxima in the scale space. In contrast, if the region saliency is measured by Laplacian-of-Gaussian function (Eqn. 1.3) in the scale space, local extrema in the scale space can be more precisely defined.

$$LoG(X, \sigma_I) = \sigma_I(L_{xx}(x, \sigma_I) + L_{yy}(x, \sigma_I)), \tag{1.3}$$

where L_{gg} denotes the second order derivative in direction g. As a result, for Harris-Laplacian detector, instead of measuring saliency of each pixel by Eqn. 1.2 alone, Eqn. 1.3 is applied on each pixel also. This process has been repeated in multiple scales (by increasing σ_I constantly and discretely) and multiple octaves. The final key-points are localized in X-Y space where Eqn. 1.2 attains local maxima and Eqn. 1.3 attains local extrema simultaneously.

Comments The search in scale space can be viewed as a simulation of viewing objects from different distances by human being. The local extrema in the scale space corresponds to the scale from which the object has been captured as a uniform and distinctive local structure. According to [7], choosing Eqn. 1.3 as the saliency function in scale space is more or less empirical.

1.2 Hessian and Hessian-of-Laplacian Detectors

Different from Harris detector, given Hessian matrix for point X:

$$H(X, \sigma) = \begin{bmatrix} L_{xx}(X, \sigma) & L_{xy}(X, \sigma) \\ L_{xy}(X, \sigma) & L_{yy}(X, \sigma) \end{bmatrix}, \tag{1.4}$$

where σ is the Gaussian smoothing parameter. Eqn. 1.6 defines the saliency of point X solely based on the determinant of Hessian matrix.

$$\mathcal{H}(X, \sigma_D) = \begin{bmatrix} L_{xx}(X, \sigma_D) & L_{xy}(X, \sigma_D) \\ L_{yx}(X, \sigma_D) & L_{yy}(X, \sigma_D) \end{bmatrix} \tag{1.5}$$

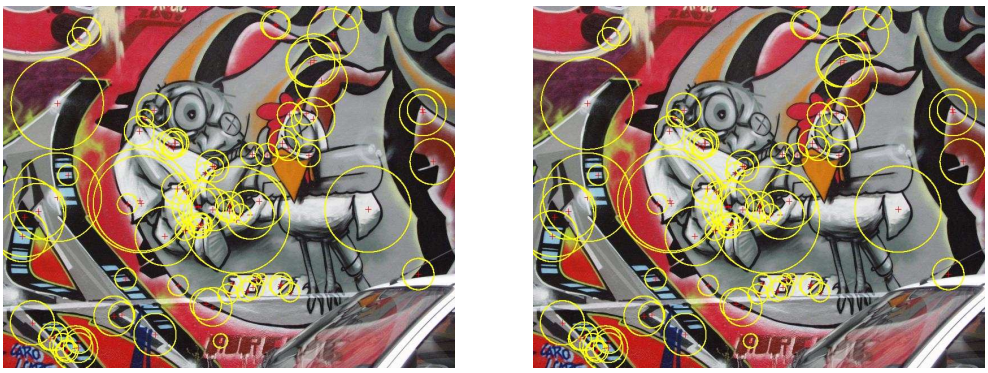

(a) the 1st (b) the 4th

Figure 1.1: Hessian points on Graffiti sequence.

Similar to Harris-Laplacian, selecting proper σ_D is required. This involves the construction of scale space with Eqn. 1.5. Hessian points are therefore defined at which Eqn. 1.5 attains local extrema in spatial and scale space.

Actually, to select proper σ_D in the scale space, we have another choice, namely, the Laplacian-of-Gaussian function, which also works well. If the detected points are required to attain local extrema with Eqn. 1.3 in the scale space, we come out a new detector: Hessian-of-Laplacian.

$$Hessian(X, \sigma) = det(H(X, \sigma)) \times \sigma^4 \tag{1.6}$$

Comments Notice that Eqn. 1.3 is shared by Harris-Laplacian and Hessian-Laplacian, while Eqn. 1.5 is shared by Hessian and Hessian-Laplacian detectors. As a consequence, it is not surprising that keypoints obtained from different detectors might be overlapping to some extent.

1.3 Laplacian of Gaussian

The saliency measurement for Laplacian-of-Gaussian is based on Eqn. 1.3. The points which attain local maxima on Eqn. 1.3 in their spatial and scale spaces simultaneously are selected. Comparing to Harris-Laplacian and Hessian-Laplacian, the saliency function in X-Y space has been replaced with Laplacian-of-Gaussian. While the saliency function in scale space keeps the same time. For this reason, they might share similar feature points.

1.4 Difference of Gaussian

The computation cost of Eqn. 1.3 turns out to be relatively high since it involves estimation of the second derivatives in x and y directions. A more efficient way is to approximate LoG via Difference of Gaussian (DoG) [2] which only requires convolving images in a constant manner (as indicated in Eqn. 1.7).

$$D(x, y, \sigma) = L(x, y, k\sigma) - L(x, y, \sigma), \tag{1.7}$$

(a) Graffiti (the 1st) (b) Graffiti (the 4th)

Figure 1.2: Fast Hessian points on Graffiti sequence [9].

where σ is the Gaussian smoothing parameter and k is an integer multiplier. David G. Lowe [2] demonstrates the effectiveness of this approach. Although *DoG* is computationally efficient, localization precision in both spatial and scale space has been sacrificed. To alleviate this issue, *Taylor expansion* on Eqn. 1.7 is adopted to approximate the exact local extrema. This scheme turns out to be quite successful. In [1], K. Mikolajczyk and C. Schmid also show that *DoG* detector outperforms *LoG* based detectors in terms of speed efficiency. As indicated later, the repeatability score of DoG detector is also pretty high.

1.5 Fast Hessian

Fast Hessian is the detector of SURF feature [12]. Its basic idea is to calculate Eqn. 1.6 in an efficient way with the help of integral images. To allow fast calculation, Eqn. 1.6 has been approximated by Eqn. 1.8.

$$Det(H_{approx}) = D_{xx}D_{yy} - (0.9D_{xy})^2, \tag{1.8}$$

where D_{xx}, D_{yy} and D_{xy} all can be calculated efficiently using box filters. Follow the way described in the note [14], we further normalize Eqn. 1.8 by the size of box filter. Notice that, this operation does not transform a non-extrema into a local extrema. It only changes the saliency score of a keypoint. Following the original implementation, the detection is performed in four scales and three octaves. Due to the considerable loss in the approximation, keypoint localization in either X-Y or scale space cannot be precise. Similar to DoG detector, *Taylor expansion* on Eqn. 1.8 is adopted to approximate the exact location of the extrema. In the original SURF implementation, the detector has been coupled with SURF descriptor for speed concern. However, it is not necessary if time cost is not the first priority. In **LIP-VIREO**, Fast Hessian in combination with SIFT descriptor demonstrates fairly stable performances in various contexts.

1.6 Dense Sampling

Dense sampling has shown considerably better performances over well designed detectors in object detection tasks. In version 1.06 and later, we incorporate implementation of dense sampling. It samples pixels in multiple scales and multiple octaves. The default sampling rate is one point for every 10 pixels. However, user is allowed to specify it in the configuration file by set 'step=n', where n is an integer larger than zero. Once it has been set, sampling rate becomes one point for every n pixels.

1.7 Affine Estimation

In order to adapt to the local structures, detectors like Harris-Laplacian, Hessian-Laplacian and Laplacian-of-Gaussian provide affine estimation for detected keypoints. Particularly, for Harris-Laplacian, the estimation is based on Eqn. 1.2 and while for Hessian-Laplacian and Laplacian-of-Gaussian, the affine region is estimated by Eqn. 1.5. Note that, we do not fully adopt iteration procedure described in [1] for the affine adaptation. Current implementation is equivalent to only one round of iteration presented in [1].

To enable the affine estimation in **LIP-VIREO**, user is suggested to set '**affine**=yes' item in the configuration file. With this setting, **LIP-VIREO** outputs the three parameters for the affine region in the ".key" file. They are a, b and c, with which an affine matrix is defined (Eqn. 1.9). Accordingly, based on this setting the descriptor is calculated in the affine region centering around the keypoint. According to our observation, keypoint features with affine adaptation show few performance difference comparing with the one without the adaptation. Notice that this observation might change when it is tested in different contexts.

$$A = \begin{bmatrix} a & b & 0 \\ b & c & 0 \\ 0 & 0 & 1 \end{bmatrix} \tag{1.9}$$

1.8 'non' detector

The integration of 'non' detector is an effort in responding to the requirements from couple of users, who are wishing to detect keypoint by themselves. The keypoints are supplied to **LIP-VIREO** for extracting the descriptors from images or displaying keypoints on the images. The 'non' detector by itself does nothing more than loading keypoints from the user specified location (specified by '**-kpdir** *path*' option). Please be noted that the input keypoint file must be suffixed with ".keys" and subject to the format shown in Appendix III.

1.9 Affiliated Properties of keypoint

Characteristic Scale For all the scale invariant detectors, each keypoint is assigned with a scale, which regularizes a canonical region centering around the keypoint. The descriptors extracted within this region will achieve scale-invariance. In the keypoint visualization, user is provided with the option to display this scale (circle or ellipse) around the keypoint. This information might be useful in various contexts. For instance, in similar/near-duplicate image retrieval, it can be leveraged in fast geometric verification as demonstrated in [16, 17].

Sign of *LoG* For all the scale invariant detectors we discussed so far, two functions are adopted to achieve scale invariance, namely, they are Laplacian-of-Gaussian (Eqn. 1.3) and Hessian Eqn. 1.5. For LoG, as discussed in [12], the sign of Eqn. 1.3 implies different local structures. In terms of Hessian function (Eqn. 1.5), although Eqn. 1.3 is not on the shelf, only few extra efforts are required to derive Eqn. 1.3 when the second order derivatives are ready.

In general, the sign of Eqn. 1.3 reflects the direction of gradient flow either pointing outward or inward. As a result, structure with negative sign will never match to structure with positive sign in Eqn. 1.3. This simple fact leads to a good property which is helpful in many contexts. For instance, in keypoint matching, computation costs can be reduced if we restrict that one patch can only match to another patch with the same sign. At the same time, the false matching rate is expected to reduce to its half. As a consequence, the sign of Laplacian turns out to be an additional property available to all the scale invariant detectors that are discussed here. User can refer to Section 3.1 for more operational details.

1.10 Performance Evaluation on Detectors

The effectiveness of local features towards recognizing objects under different degree of transformations has been surveyed in [4]. In this section, we conduct similar studies to compare the recognition effectiveness of different keypoint detectors. The following evaluations are conducted based on the image sequences and testing software provided by K. Mikolajczyk [4].

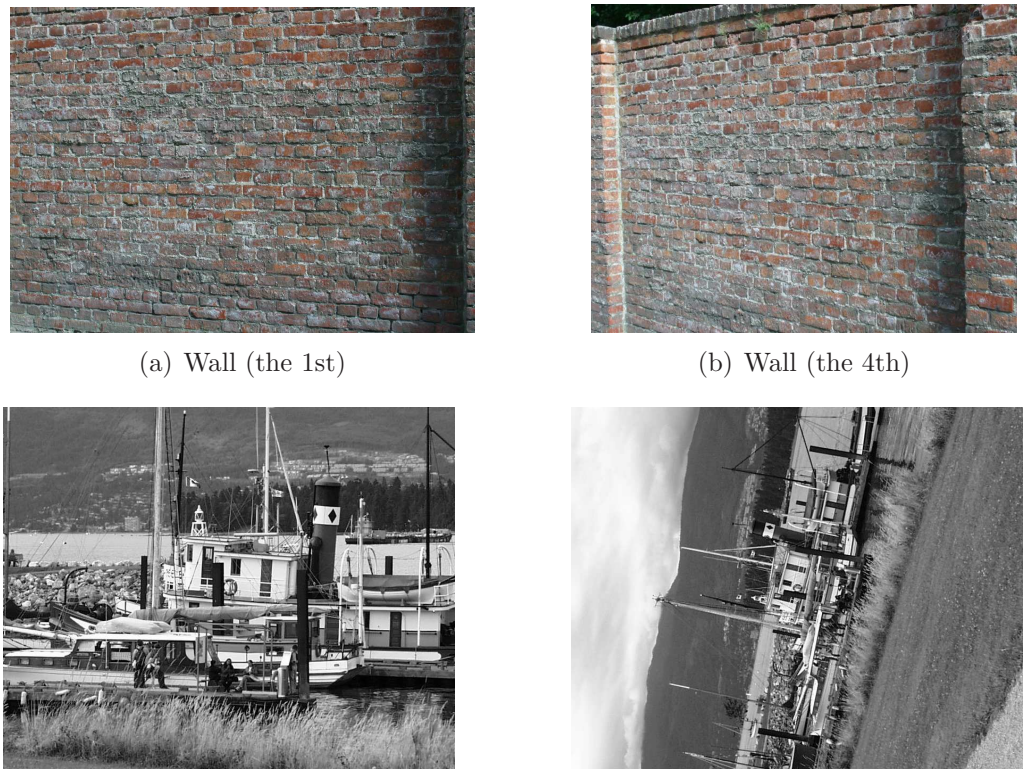

(a) Wall (the 1st) (b) Wall (the 4th)

(c) Boat (the 1st) (d) Boat (the 4th)

Figure 1.3: Image samples that have been adopted in performance evaluation.

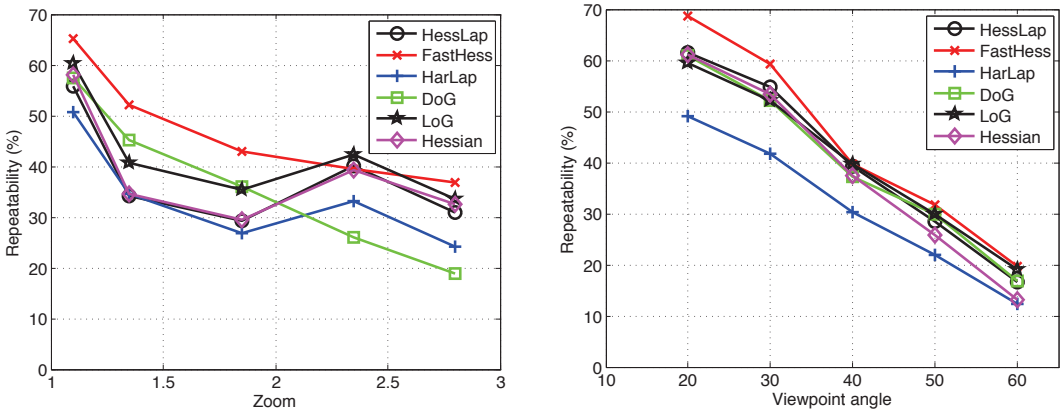

(a) Incremental scale changes on Boat series (b) Incremental viewpoint changes on Wall series

Figure 1.4: Performance of Difference-of-Gaussian, Harris-Laplacian, Hessian-Laplacian, Fast Hessian, Laplacian-of-Guassian using detectors extracted by LIP-VIREO.

Chapter 2

Descriptors

Once keypoints have been localized in the X-Y and scale spaces, we are able to see what these local structure look like. However, it is still not enough if one wants to take these keypoints to represent an image. For instance, we are yet ready to compare two images with keypoints since keypoint on itself cannot be discriminative. This is where the descriptor comes to fit in. In general, the descriptor helps to convert an intensity map centering around the keypoint into a feature vector. This vector in turn can be used for comparison under various situations.

There are ten descriptors that have integrated in **LIP-VIREO**. They are SIFT and its variants, namely, flip invariant SIFT (F-SIFT), PCA-SIFT and FIND. Moreover, one can also find implementation of descriptors such as SURF, AoD, SPIN, RIFT, ERIFT and Steerable Filters in the package. In the following sections, we review these descriptors and our implementation in brief. In the last section, a brief evaluation on these descriptors is presented. The instructions on how to choose among descriptor options provided by **LIP-VIREO** in the command line can be found in Section 3.2.

2.1 SIFT

SIFT has been shown to be successful in various tasks such as object classification, panorama generation, wide baseline matching and ND image identification. Given a normalized keypoint patch, SIFT generates a 2-D histogram on the local patch. The local patch has been partitioned into blocks. Figure 2.1 shows the partition scheme of SIFT. Gradient of a pixel within each partition block has been quantized according to its orientation. Typically, the number of quantization bins is 8. According to [2], this setting reaches to the best performance. Before the quantization, this local patch is rotated to its dominant orientation. This operation enables the extracted feature to be invariant to rotation transformation. The dominant orientation is estimated also based on orientation quantization in the gradient field of this local patch. Usually, the region used for dominant orientation calculation is small portion of the local patch (e.g., concentric region of the patch with half radius length). To achieve better performance, the histogram are further weighted firstly by its gradient length, secondly by a Gaussian window centering around the keypoint. Our implementation of SIFT is every bit like

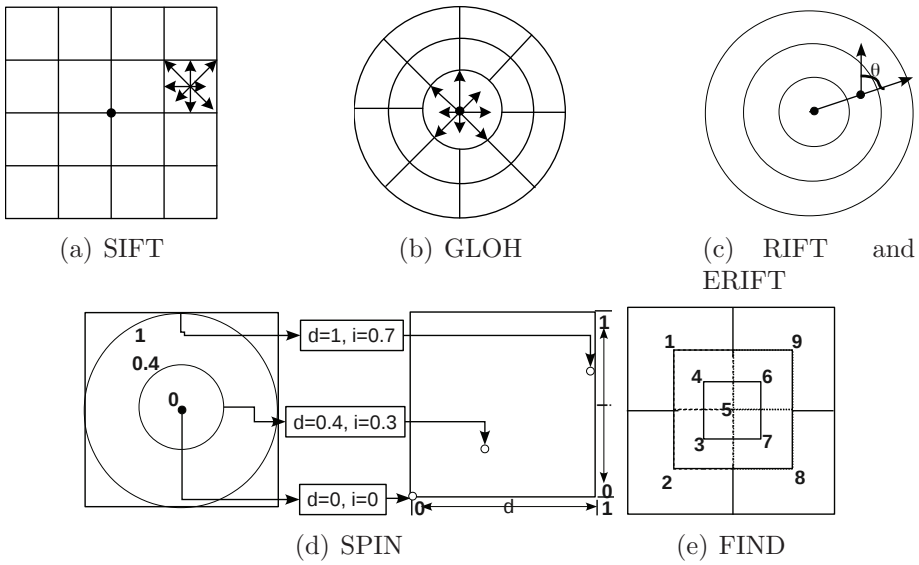

(a) SIFT (b) GLOH (c) RIFT and ERIFT

(d) SPIN (e) FIND

Figure 2.1: Partition schemes for SIFT, GLOH, RIFT and ERIFT.

what described in [2], except that we normalize the patch with Gaussian smoothing before the quantization. This operation turns out to be rewarding. Another interesting variant of SIFT is GLOH which applies a log-polar partition on the local patch (shown in Figure 2.1(b)).

2.2 Flip invariant SIFT

In version 1.06 and later, the flip invariant SIFT is incorporated, which is proposed by us. This new descriptor is able to maintain similar performances as SIFT feature for cases flip is not involved, while it outperforms SIFT apparently on the cases that flip operation is observed. One is referred to our recent technical report [15] for more details.

2.3 PCA-SIFT

PCA-SIFT is another variant of SIFT. Instead of quantizing the gradient field, it maps the gradient field to a vector (typically *36* dimensions) with a trained PCA matrix. Before performing the mapping, the local patch is normalized to fixed size (e.g., 41×41) patch. Gradient of each pixel in the normalized patch is calculated. These gradients (including radius length and orientation) are then concatenated one after another from the up-left to bottom-right. This results in a long vector (twice of the number of pixels). This long vector is mapped to relatively low dimension (e.g., *36*) via a PCA mapping matrix. The mapping matrix is learned from several thousands of local patches in advance. In **LIP-VIREO**, the implementation from Yan Ke is fully incorporated. For integrity, we keep all its default settings. Such that the mapping matrix available from PCA-SIFT website is still valid.

2.4 FIND

FIND [18] is proposed as a variant of SIFT which is enabled with flip invariance. Similar to SIFT, histogram on gradients is generated. The major difference of FIND from SIFT lies in the partition scheme, which allows overlapping between blocks (as shown in Figure 2.1(e)). As indicated in the figure, the number of pixels is not distributed evenly in each block. The flip invariance is achieved by first characterizing patches as either left-pointing or right-pointing. A flip indicator (left or right) is thus kept in the descriptor for each patch. when a left-pointing patch matches with a right-pointing patch, feature vector from one of them is reversed. Then the flip invariance is actually achieved during the matching. In our implementation, we find such kind of indicator is unnecessary once if we normalize (flip) the patch to one orientation (e.g., left-pointing). As a result, FIND becomes quite similar to F-SIFT except they rely on different information for flip normalization and they adopt different partition schemes. Comparing with F-SIFT, either the partition scheme or orientation estimation adopted by FIND is less stable. In terms of computation cost, the latter is cheaper.

2.5 Steerable Filters

Steerable filters has been used in many contexts. It is also known as local jet or textons. They are partial derivatives obtained by applying series of Gaussian kernels on the local patch. In **LIP-VIREO**, we follow the implementation described in [4] in which a 41×41 Gaussian window centering around the keypoint is adopted. The derivatives have been calculated up-to the forth order. This results in a 15-dimensional feature vector which includes intensity value of the pixel itself and different order of derivatives. They have been arranged in following order.

v, dx, dy, dxx, dxy, dyy, $dxxx$, $dxxy$, $dxyy$, $dyyy$, $dxxxx$, $dxxxy$, $dxxyy$, $dxyyy$, $dyyyy$

2.6 SPIN

The intensity domain SPIN image incorporated in **LIP-VIREO** is a two-dimensional histogram encoding the distribution of image brightness values in the neighborhood of a particular reference (center) point. The quantization scheme is illustrated in Figure 2.1(d). The implementation is every bit like the description in [6]. The two dimensions of the histogram are d, distance from the center point, and i, the intensity value. The "slice" of the spin image corresponding to a fixed d is simply the histogram of the intensity values of pixels located at a distance d from the center. Since the d and i parameters are invariant under orthogonal transformations of the image neighborhood, spin images offer an appropriate degree of invariance for representing affine normalized patches. In our implementation, we choose *10* bins for distance and another *10* histogram bins for the intensity levels, which results in an 100-dimensional feature descriptor.

In **LIP-VIREO**, the SPIN image is implemented as a "soft histogram", where each pixel within the support region contributes to more than one bin. Specifically, the contribution of a pixel located in x to the bin indexed by (d, i) is given by Eqn. 2.1.

$$exp(-\frac{(|x-x_0|-d)^2}{2\times\alpha^2}-\frac{(I(x)-i)^2}{2\times\beta^2}), \tag{2.1}$$

where x_0 is the location of the center pixel, and α, β are the parameters representing the "soft width" of the two-dimensional histogram bin. Note that the soft histogram can be seen as a set of samples from the Parzen estimate (with Gaussian windows) of the joint density of intensity values i and distances d.

According to our observation, SPIN shows excellent performances in the context that only rotation and flip transformations are involved. The performance drops dramatically when it faces images with scale transformation. In addition, extracting SPIN feature could be very slow (roughly 10 times slower than that of SIFT).

2.7 SURF and AoD

In general, SURF descriptor shares the same partition scheme as SIFT. However, in each block, in stead of generating histogram on gradients, SURF aggregates on Haar wavelets of different channels. Similar as SURF detector, box filters are exploited for speed efficiency. The aggregation is performed on dx, $|dx|$, dy and $|dy|$. This results in a *64* dimensional vector. In the original paper, a variant of SURF which separates the negative wavelets from the positive ones was presented. This allows a few improvement over original version. However, this flexibility is not incorporated in our implementation.

The proposal of AoD is inspired by SURF descriptor. Comparing with SURF, the only difference lies in the box filters. In AoD the box filters have been replaced with derivatives in each pixel. Due to the higher cost in calculating derivatives, AoD turns out to be less efficient than SURF.

We evaluated our SURF implementation by matching near-duplicate image pairs. However, the performance is unsatisfactory. The performance difference can be attributed to difference in implementation details which cannot be found in the paper [12] or inappropriate parameter tuning. Currently, the performance from Fast Hessian combined with SURF cannot compete with the original implementation. For this reason, if one wants to perform evaluation related to SURF in his scientific study, choosing the original implementation is strongly recommended. Nevertheless, when *Fast Hessian* combined with other descriptors such as *SIFT* or *F-SIFT*, it performs fairly well. It is safe to choose this combination if speed efficiency is not the major concern.

2.8 RIFT and ERIFT

To obtain a complementary representation of local appearance of normalized patches, Lazebnik and et. al have developed a rotation-invariant descriptor that generalizes Lowe's SIFT [2]. The normalized circular local patch has been partitioned into concentric rings (as shown in Figure 2.1(c)). Rings share the same width. For this reason,

different ring covers different number of pixels. In other word, the sizes of histogram are different. Apparently, the outer rings have larger coverage. To maintain rotation invariance, this orientation is measured at each point relative to the direction pointing outward from the center. We use four rings and eight histogram orientations. It therefore yields 32-dimensional descriptors.

ERIFT is short for Enhanced Rotation Invariant Feature Transform. It is an enhanced version of Rotation Invariant Feature Transform [6]. ERIFT follows the same partition scheme as RIFT on a local patch. But different from RIFT, we carefully set the width of each ring, to make sure these rings cover equal number of pixels. Similar to RIFT, the gradient orientation histogram is computed within each ring. To maintain rotation invariance, this orientation is measured at each point relative to the direction pointing outward from the center. We use eight rings and eight histogram orientations. In order to make it more distinctive, the quantization is performed on two perpendicular directions for each gradient value. It finally yields 128-dimensional descriptors. To enable flip invariance, for each pixel, in addition to quantizing along its gradient direction, we quantize it to the flipped gradient direction. ERIFT demonstrates better performance than RIFT in general cases when scale transformation is observed.

Comments Comparing with SIFT descriptor, both RIFT and ERIFT loose the geometric constraint on pixels, especially, along the log-polar direction. This enables RIFT and ERIFT to be invariant to both flip and rotation. However, as a side-effect, pixels are free to move around along the log-polar direction, while the final representation of RIFT or ERIFT keeps the same all the time. For this reason, the distinctiveness of the descriptors has been undermined. According to our observation, neither RIFT nor ERIFT can be as discriminative as SIFT feature.

2.9 Performance Evaluation on Descriptors

We evaluate seven different visual descriptors including SIFT, PCA-SIFT, F-SIFT, FIND, SPIN, MI-SIFT (Mirror and Invert invariant SIFT [13][1]) and SURF for investigating their accuracy in keypoint matching. Similar to [12], a set of image pairs are sampled from the eight image sequences for experiment. The set includes the first and fourth images from each sequence. In addition to the original transformations (blur, rotation, zoom, change of lighting, color and JPEG compression rate) in the image set, flip transformation is included by flipping the fourth image of each sequence. In the experiment, except SURF, DoG detector is employed for all the visual descriptors. Following with [4], the performance evaluation is measured by assessing the number of point-to-point matches being correctly returned. Figure 2.2 shows the performance in terms of recall-precision curve averaged over the results on eight image pairs.

[1]Code is shared from the author.

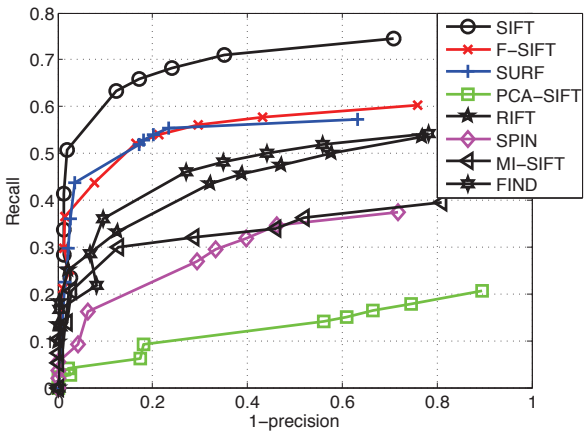

(a)

Figure 2.2: Performance of eight different descriptors with DoG detector on *8* image pairs which cover transformations such as scale, rotation, viewpoint changes, blur, changes in JPEG compression rate and lighting changes. Notice that performance of SURF is from its original implementation.

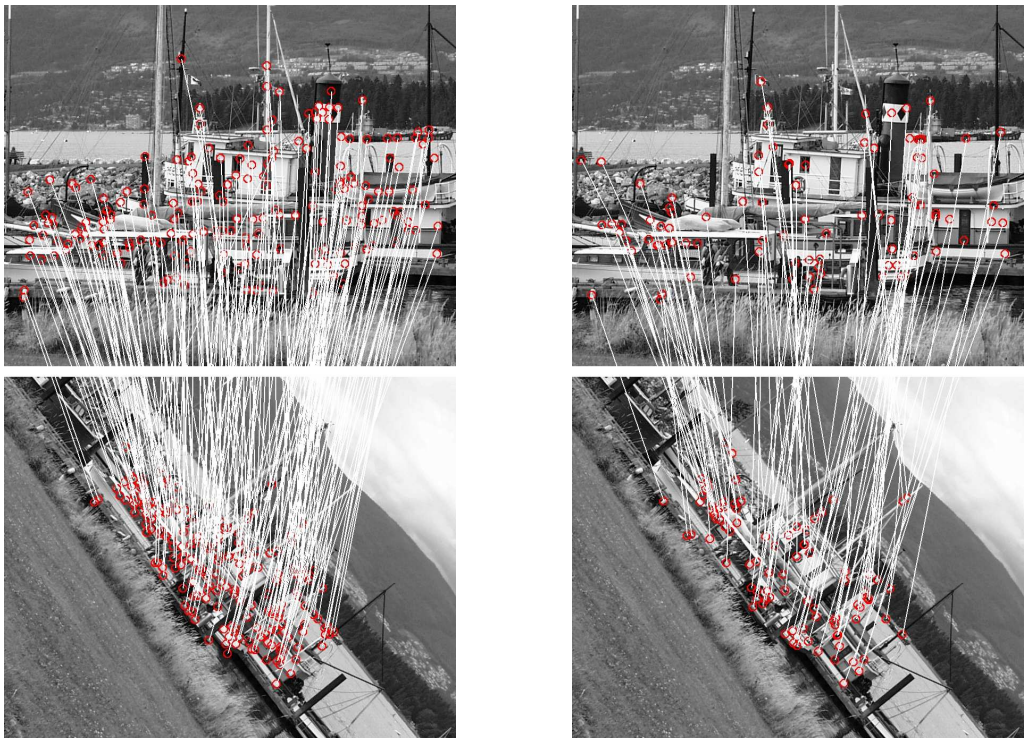

(a) DoG+SIFT, the 1st matches to the 2nd

(b) Hessian+SIFT, the 1st matches to the 4th

Figure 2.3: One-to-one and Symmetric matching on Graffitti sequence with DoG and Hessian detectors.

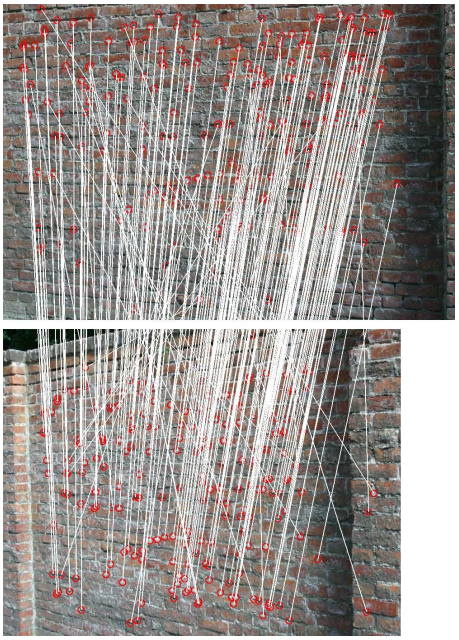

(a) DoG+SIFT, the 1st matches to the 2nd

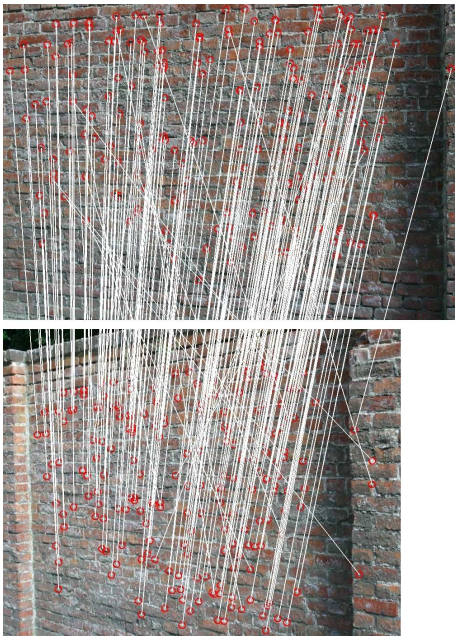

(b) Hessian+SIFT, the 1st matches to the 4nd

Figure 2.4: One-to-one and Symmetric matching Wall sequence with DoG and Hessian detectors.

Chapter 3

Command Line Options

3.1 Keypoint detection

Command below extracts keypoints from input image or images specified by *path*.

lip-vireo [**-img**|**-dir**] path **-d** [`dog`|`hess`|`harr`|`ykpca`|`log`|`harlap`|`hesslap`|`mser`|`dsurf`|`dense`|`non`] [**-kpdir**] path **-c** file.conf

- **-img** `path`
- **-dir** `path`

For the above two options, only one can be selected at once. For '**-dir**' option, **LIP-VIREO** batchfully extracts keypoints for each image under folder '*path*', while option '**-img**' processes only one image (given by '*path*') at once. Currently, the program only accepts images formatted in '**pgm**', '**ppm**', '**bmp**' and '**jpg**'. **Notice that, the file name should be suffixed with '*.pgm*', '*.ppm*', '*.bmp*' and '*.jpg*' correspondingly, otherwise, image will be simply ignored by the program.**

- **-d** [`hess`|`harr`|`dog`|`ykpca`|`log`|`harlap`|`hesslap`|`mser`|`dsurf`|`dense`|`non`]

This option is always required, it allows user to choose among detectors such as Harris ('`harr`'), Hessian ('`hess`'), Hessian-Laplacian ('`hesslap`'), DoG ('`dog`'), Laplacian of Gaussian ('`log`'), Harris-Laplacian ('`harlap`'), Fast Hessian ('`dsurf`'), Dense sampling ('`dense`') and PCA-SIFT ('`ykpca`') implemented by Yan Ke. For all these detectors, only Harris is not scale-invariant since it only localizes the keypoint in X-Y space.

For '`ykpca`' option, **LIP-VIREO** outputs keypoints along with PCA-SIFT descriptors. For this option, user is required to append one item '*pcamat* = *pcamat_path*' in the configure file 'file.conf', to specify the path for PCA matrix file. The format of the file is the same as Yan Ke provided (user can download it from PCA-SIFT website).

For detector '`dense`', this tool simply samples the pixels on the image densely. By default, one pixel is chosen for every 10 pixels. This default setting can be reset by put 'step=n' in the configuration file. Once it has been re-configured, the sampling rate becomes one point for every n pixels.

By specifying '`non`' detector, one is allowed to input keypoints detected by his own algorithms for display or descriptor extraction. When this special detector is selected, the '-kpdir' **MUST BE** specified to point out where user's keypoint files located.

- **-kpdir** `path`

Option '**-kpdir**' is used to indicate the destine directory where the features are saved. By default, the output keypoints file has the same name as the input image but with different suffix. We fix the suffix to '.keys'. It is a text file. Each line in the file writes in following format.

x_cord y_cord a b c iscale angle score

One line in the resulting file gives description for one keypoint. There are totally 8 items and are arranged in 8 columns. 'x_cord' and 'y_cord' are basically x and y location of the keypoint. 'a', 'b' and 'c' are parameters for the adapted affine region (ellipse shape). 'iscale' is the detected integration scale for the point. 'angle' indicates the dominant orientation of the local patch around the keypoint. While 'score' is the function value of detected point according to specified detector. In general, this value indicates the saliency of one keypoint, the higher of this value the more salient the point is.

- **-c** file.conf

This option is always required. In configuration file 'file.conf', several settings for additional options are provided. It is formatted as follows.

option1=value1
option2=value2

Item before '=' (e.g. 'option1') is the option to be specified, setting is put after '='. Valid values can be assigned to the corresponding option. Configuration on five options, '**pcamat**', '**topk**', '**scale**', '**angle**' and '**affine**', are explained as follows. While the complete list of available options are shown in Table 3.1.

Option '**pcamat**' allows user to set the path for PCA mapping matrix when 'ykpca' is chosen for '-d' option. To specify it, user should use '**pcamat**=path'. Option 'topk' allows user to specify the maximum number of keypoint that returns from one image. Once '**topk**' has been set, detector tries to choose top '**topk**' number of keypoints according to their saliency scores. When '**scale**' option is specified to 'yes', **LIP-VIREO** outputs the characteristic scale detected for each keypoint to the descriptor file. Similarly, when '**angle**' option is specified to 'yes', **LIP-VIREO** outputs the dominant orientation estimated for each keypoint to the descriptor file. Noted that 'scale' and 'angle' are options for descriptor extraction. For keypoint detection option '-kpdir', the scale and dominant orientation will be generated despite these two options are enabled or not.

Different from 'scale' and 'angle' options, 'affine' option takes effect for keypoint detection, descriptor extraction and keypoint display. When it is set to 'yes', detector

Table 3.1: Check List of Available Options for Configuration

Option	Value	Default value	Take effect with option(s)
scale	yes/no	no	'-d *'
angle	yes/no	no	'-d *'
topk	integer (> 0)	750	'-d *'
pcamat	string (path of PCA matrix)	empty	'-d ykpca'
step	integer (> 0)	10	'-d dense'
circle	yes/no	no	'-drdir'
affine	yes/no	no	'-d *', '-p *', '-drdir'
format	vireo/vgg	vireo	'-d *', '-p *'
log	string (path of log file)	empty	'-d *', '-p *'

*: applies to all available choices for the option.

estimates the affine region for each keypoint. Note that for the detectors, such as 'DoG', 'dsurf' and 'harr', which do not support affine adaptation, **LIP-VIREO** simply outputs an identity matrix. Finally, the detected affine regions will be outputed to keypoint files ('.keys') and the descriptors will be extracted from an ellipse instead of from a circle region. If '-drdir' option is specified, keypoints are displayed with ellipse scales in the image.

In current versions, an empty configuration file must be provided even user doesn't prepare to use any additional settings.

3.2 Descriptor extraction

Command as follows extracts descriptors from image or images.

lip-vireo [**-img**|**-dir**] path **-d** [*detector*] **-p** [$SIFT|LJET|SPIN|ERIFT|FIFT|FIND|SURF|AOD$] [**-dsdir**] path **-c** file.conf

Settings for options '**-img**', '**-dir**', '**-d**' and '**-c**' are the same as keypoint detection. So please refer to Section 3.1 for details. The focus of this section is on descriptor options: '**-p**' and '**-dsdir**'.

First of all, for descriptor extraction, a proper detector must be chosen for '**-d**'. This time, option '-kpdir' becomes optional. However, there is one exception. When detector option is set to '-d non', '-kpdir' is required to specify, i.e., user has to offer **LIP-VIREO** with the location of keypoint file(s). At the same time, one has to make sure the file is correctly formatted (refer to Appendix III) and the file name is suffixed with '.keys'.

- **-p** `SIFT|LJET|SPIN|ERIFT|FIFT|FIND|SURF|AOD`

In addition, one is required to specify the descriptor by '-p'. Available choices are SIFT, FIFT, RIFT, ERIFT, SPIN, SURF, AoD and LJet (Local Jet feature). User is free to choose either normalized the descritpors (l_2 norm) or features. To generate normalized

descriptor, one can put character 'N' before the wanted descriptor option. For example, if '-p SIFT' is set, raw SIFT feature will be generated. Alternatively, if '-p NSIFT' is specified, **LIP-VIREO** outputs normalized feature vector.

- **-dsdir** `path`

Corresponding to '**-img**' and '**-dir**' options, '**-dsdir**' option specifies destine directory where to save the keypoint descriptor files.

By default (if 'affine=yes' is not specified in the configuration file), the descriptor is calculated within a circle region centering around the keypoint. Otherwise, the descriptor is calculated within a normalized affine region.

In addition to descriptor for each keypoint, in the descriptor file, user is allowed to keep affiliated information such as scale and rotation along with each detected keypoint. To achieve this, user needs to put following configurations in the configure file before the detection.
#output scale
scale=yes
#output angle
angle=yes
Similar to location 'x' and 'y', 'scale' and 'angle' are treated as affiliated properties of one keypoint and have been placed right after 'x' and 'y'. **Note that when user chooses to output scale and angle together, the output order for these two properties in the descriptor file is fixed to <scale, angle>.** For the format of the descriptor file, see details in Appendix I.

3.3 Visualization

3.3.1 Display Local Interest Point on the Image

In version 1.05 and later, user is allowed to display the keypoints on the input image with both location (with a cross in red) and the region (with an ellipse in yellow). The command is as follows.

lip-vireo [**-img**|**-dir**] path **-d** [`dog`|`hess`|`harr`|`ykpca`|`log`|`harlap`|`hesslap`|`dsurf`|`dense`|`non`] [**-kpdir** kpdir] **-drdir** imgdir **-c** file.conf

As shown in the command, in order to display points on the image(s), user has to specify the option '`-drdir`' to indicate where to save the image(s) with keypoints plotted. Actually, this option also invokes the displaying routine. Other options are the same as keypoint detection.

Note that the local interest point regions that are displayed can be either in circle or ellipse depending on both the option for detector and whether setting 'affine=yes' has been enabled in the file 'file.conf'. For instance, for detectors 'harlap', 'hesslap' and 'log', the regions are displayed in ellipses only when the setting 'affine=yes' has

been set. For detector 'dog', the plotted regions are circles all the time since no affine estimation available with it. For Fast Hessian, the regions are displayed with squares all the time, which follows the tradition of original implementation. Similar to original implementation, the square is rotated to its dominant orientation as well.

In version 1.06 and later, user is allowed to display keypoints with 'cross' only or 'cross' along with 'circle'. By default, only crosses are plotted in the image. In order to display local region with circle (or ellipse), user is required to specify 'circle=yes' in the configuration file.

For detector option '-d non', user MUST specify option '-kpdir' to point out the location of keypoint file(s). while for other detector options, '-kpdir' is optional.

3.3.2 Display Local Patches in Rows and Columns

In version 1.26 and later, user is allowed to display the detected keypoints in one image. The patches are extracted centering around the keypoint and normalized (to 41×41 patch) with its characteristic scale. The command is as follows.

lip-vireo [**-img**|**-dir**] path **-d** [`dog`|`hess`|`harr`|`ykpca`|`log`|`harlap`|`hesslap`|`dsurf`|`dense`|`non`] **-dvdir** dstdir **-c** file.conf

As shown in above command, function of displaying keypoint patches can be specified by '**-dvdir** dstdir' option. Once it has been chosen, all the detected keypoints from the input image will be displayed in one image. The normalized patches are organized into columns and rows. The image(s) is/are saved to 'dstdir'. Normalized patches of Harris-Laplacian, Fast Hessian, Hessian and Hessian-Laplacian points are shown in Figure 3.1(c), (d), (g) and (h) respectively.

(a) Harris-Laplacian points

(b) Fast Hessian points

(c) Normalized Harris-Laplacian patches

(d) Normalized Fast Hessian patches

(e) Hessian points

(f) Hessian-Laplacian points

(g) Normalized Hessian patches

(h) Normalized Hessian-Laplacian patches

Figure 3.1: Display of keypoints from various detectors and their corresponding patch views. They are obtained with option: '-drdir dstdir' and '-dvdir dstdir' respectively.

Chapter 4

MISC

4.1 Important Notice

Features extracted by **LIP-VIREO** are not necessarily compatible with the features derived from tools by VGG [9], Prof. D. G. Lowe [2] or Dr. Dorko [11]. Therefore, the performance is not guaranteed when there is any mixture use of these detectors or descriptors.

4.2 Copyright

4.3 Acknowledgements

We would like to express our sincere thanks to Dr. Yan Ke from CMU, USA who provides us PCA-SIFT source code. His assistance has been invaluable. We are very grateful to Dr. Dorko from Technical University Damstadt, Germany who sends us many suggestions about how the dominant orientation of local patch is estimated. Gratefulness also reaches to Mr. Xiao-Jie Guo from University of Tianjin, China, whose informative suggestions and patience help the implementing of FIND. Great thanks also reach to Dr. Rui Ma from IBM, China who kindly shares us the matlab implementation of MI-SIFT.

4.4 Release Notes

4.4.1 V1.26 Release Note

1. Fast Hessian detector has been integrated.
2. SURF descriptor has been integrated. (find more details in Section 2.7)
3. SURF-like descriptor 'AoD' (Aggregation on the first order Derivatives) has been integrated. (find more details in Section 2.7)
4. User is allowed to display keypoint as patches. (find more details in Section 3.3.2)
5. DoG detector has been optimized.
6. SIFT-like Flip invariant descriptor FIND has been integrated. (find more details in Section 2.4)
7. Bug that causes exceptions during loading PPM image has been identified and removed.
8. Detector **mser** has been removed for its unstable performance.

4.4.2 V1.067 Release Note

1. The performance of detector 'hess' has been optimized. It is able to achieve similar performance as 'hesslap' (hessian-laplacian).

4.4.3 V1.06 Release Note

1. The 'dense' detector has been integrated (check more details in Section 1.6).
2. 'ppm' formatted images are supported.
3. Flip invariant SIFT descriptor is integrated (check more details in Section 2.2).
4. In, keypoint feature display, user is enabled to either display 'cross' only or display 'cross' along with 'ellipses' (check more details in Section 3.3.1).

4.4.4 V1.055 Release Note

1. The MSER detector has been integrated.
2. A bug in loading JPEG file is identified and removed.
3. The '-d non' detector option is provided, which allows user to supply his own keypoints for extracting local interest descriptors. (see more details from Section 1.8)

4.4.5 V1.05 Release Note

1. Bugs in reading bmp file under Linux have been removed.

2. Bug causes irregular output of keypoints has been removed, which impacts the performances of hesslap and dog detectors in Version 1.042 a lot.

3. Function to plot keypoints onto the input image(s) has also been integrated. Please refer to Section 3.3.1 for more details.

4.4.6 V1.044 Release Note

1. We optimized the implementation of SIFT descriptor. The gradient-orientation bins with fewer energy are smoothed to zero. As a result, the SIFT feature becomes sparser. Based on our observation, such kind of modification results in better point-to-point matching results than previous versions. Note that, because of the modification, SIFT feature generated by this version is NOT COMPATIBLE to previous versions.

4.4.7 V1.042 Release Note

1. We optimized the parameters for descriptor calculation. As a result, features generated by this version may NOT be compatible with features generated by previous versions.

2. In this new version, user can obtain the affine region a keypoint by setting "affine=yes" in the configuration file. Please check details in Section 3.1.

3. We change the output format keypoint file (NOT the descriptor file). Please check details in Section 3.1.

4.4.8 V1.03 Release Note

1. SPIN descriptor is incorporated in this new version which is invariant to rotation and flip transformation. According to our experiment, it is also partially invariant to scaling. See more details in Section 2.6.

2. A novel descriptor ERIFT (Enhanced Rotation Invariant Feature Transform) which is invariant to scale, rotation and flip transformation has been incorporated. See details in Section 2.8.

3. Binary code which can be run under SunOS is also available for this new version.

4. Minor changes have been made on notations for descriptor options. For example, to choose un-normalized SIFT, user should choose 'SIFT' instead of 'UNSIFT'. Accordingly, normalized SIFT option has been changed to 'NSIFT'. Similarly, option for un-normalized LJet feature is changed to 'LJET', while for the normalized the LJet feature, the option is modified to 'NLJET' See details in Section 3.2.

4.4.9 V1.02 Release Note

1. In the descriptor file, user can choose to output scale and rotation information affiliated with each keypoint after proper configurations. Please check more details from Section 3.2.

2. The output format of descriptor file has been modified. For that reason, it becomes INCOMPATIBLE with previous versions. Check more details in Section 4.4.10.

4.4.10 V1.01 Release Note

1. **LIP-VIREO** accepts 'JPEG' formatted images as input.

2. Bug causes exception when inputting gray level 'jpeg' and 'bmp' has been identified and removed.

3. Bug causes exception when choosing 'ykpca' option has been identified and removed.

4. Performance of keypoint detector 'LoG' (`log`), 'Hessian-Laplacian' (`hesslap`) and 'Harris-Laplacian' (`harlap`) have been further improved. Comparing with previous versions, they produce less number of keypoints while achieving better performances.

Appendix

I. Format of descriptor file (Version 1.02 and later)

numkp	m	d		
p_1	p_2	...	p_m	
val_1	val_2	val_3	...	val_k
val_{k+1}	val_{k+2}	val_{k+3}	...	val_{2k}
...	...	...	...	...
val_{d-k+1}	val_{d-k+2}	val_{d-k+3}	...	val_d
p_1	p_2	...	p_m	
val_1	val_2	val_3	...	val_k
val_{k+1}	val_{k+2}	val_{k+3}	...	val_{2k}
...	...	...	...	...
val_{d-k+1}	val_{d-k+2}	val_{d-k+3}	...	val_d

◇ **numkp**: the number of features in the file

◇ **m**: the number affiliated properties, such as x, y, scale and dominant orientation. Especially, for local interest features. These properties have been put in a fixed order, i.e., x, y, scale and dominant orientation. If there is no affiliated properties, **m** is set to *0*.

◇ **d**: the dimension of the feature vector. The feature vector might be put in one line or several lines. Feature values that are in same line are separated by blank characters. The name of feature file is suffixed with fixed identifier: '**.pkeys**'.

II. Format of descriptor file (Version 1.01 & 1.00)

numkp	d	$nline$		
x_1	y_1			
val_1	val_2	val_3	...	val_k
val_{k+1}	val_{k+2}	val_{k+3}	...	val_{2k}
...	...	...	...	...
val_{d-k+1}	val_{d-k+2}	val_{d-k+3}	...	val_d
x_2	y_2			
val_1	val_2	val_3	...	val_k
val_{k+1}	val_{k+2}	val_{k+3}	...	val_{2k}
...	...	...	...	...
val_{d-k+1}	val_{d-k+2}	val_{d-k+3}	...	val_d

◇ **numkp**: the number of features in that file

◇ **d**: the dimension of the feature vector. The feature vector can be put in one line or several lines. Values presented appear in same line are separated by blank characters. The name of feature file is suffixed with '**.pkeys**' all the time.

◇ **nline**: it indicates how many lines that the descriptor feature takes up for one keypoint besides coordinate information (x, y).

III. Format of input keypoint file for 'non' detector option (Version 1.05 and later)

numkp *col*

x_1	y_1	a_1	b_2	c_3	*scale*	*angle*
x_1	y_1	a_1	b_2	c_3	*scale*	*angle*
...	...	...	...	...	...	...
x_n	y_n	a_n	b_n	c_n	*scale*	*angle*

◇ **numkp**: the number of features in this file.

◇ **col**: the number of columns in each line.

◇ **x and y**: X and Y location of a keypoint.

◇ **a, b and c**: parameters for ellipse region, if it is a circle, it is specified as $a = 1$, $b = 0$ and $c = 1$.

◇ **scale**: the characteristic scale of a keypoint, the radius of the local patch used for extracting descriptor.

◇ **angle**: the dominant orientation of the local patch.
Please be noted that the file name MUST BE suffixed with '.keys' all the time.

Bibliography

[1] M. K. and C. Schmid, "Scale and affine invariant interest point detectors," *International Journal of Computer Vision*, Vol. 60, pp. 63–86, 2004.

[2] D. Lowe, "Distinctive image features from scale-invariant keypoints," *International Journal on Computer Vision*, Vol. 60, no. 2, pp. 91–110, 2004.

[3] Y. Ke and R. Sukthankar, "PCA-SIFT: A more distinctive representation for local image descriptors," in *Computer Vision and Pattern Recognition*, Vol. 2, 2004, pp. 506–513.

[4] K. Mikolajczyk and C. Schmid, "A performance evaluation of local descriptors," *IEEE Trans. on Pattern Analysis and Machine Intelligence*, Vol. 27, no. 10, pp. 1615–1630, 2005.

[5] C.-W. Ngo, W.-L. Zhao, and Y.-G. Jiang, "Fast tracking of near-duplicate keyframes in broadcast domain with transitivity propagation," in *ACM Multimedia Conference*, 2006, pp. 845–854.

[6] Svetlana Lazebnik, Cordelia Schmid, and Jean Ponce, "A sparse texture representation using local affine regions", in *IEEE Transactions on Pattern Analysis and Machine Intelligence*, 2005, Vol. 27, pp. 1265–1278.

[7] T. Lindeberg, "Feature detection with automatic scale selection," *International Journal of Computer Vision*, Vol. 30, no. 2, pp. 79–116, 1998.

[8] D.-Q. Zhang and S. Chang, "ND Retri. & Det. Test set," in http://www.ee.columbia.edu/ln/dvmm.

[9] A. Zissermanin and etc, "Visual Geomtry Group" in http://www.robots.ox.ac.uk/~vgg/.

[10] TREC Video Retrieval Evaluation (TRECVID), in http://www-nlpir.nist.gov/projects/trecvid/.

[11] Dorko, "Keypoint Detectors & Descriptors," in http://lear.inrialpes.fr/people/dorko/downloads.h

[12] H. Bay, A. Ess, T. Tuytelaars, and L. V. Gool, "SURF: Speeded up robust features," *Computer Vision and Image Understanding*, vol. 110, no. 3, pp. 346–359, 2008.

[13] R. Ma, J. Chen, and Z. Su, "MI-SIFT: mirror and inversion invariant generalization for SIFT descriptor," in *International Conf. on Image and Video Retrieval*, 2010, pp. 228–236.

[14] Christopher Evans: Notes on the OpenSURF Library, 2009.

[15] Wan-Lei Zhao. "A Comprehensive Study over Flip Invariant SIFT". Technical report, May. 2011.

[16] H. Jégou, M. Douze, and C. Schmid, "Hamming embedding and weak geometric consistency for large scale image search," in *European Conf. on Computer Vision*, 2008.

[17] W.-L. Zhao, X. Wu and C.-W. Ngo, "On the Annotation of Web Videos by Efficient Near-duplicate Search," *IEEE. Trans. on Multimedia*, vol. 12, no. 5, pp. 448–461, 2010.

[18] X. Guo and X. Cao, "FIND: A neat flip invariant descriptor," in *International Conf. on Pattern Recognition*, 2010, pp. 515–518.

[19] MSER Implimentation, in http://www.vlfeat.org/~vedaldi/code/mser.html

[20] VIREO, in http://vireo.cs.cityu.edu.hk.

[21] Patent of SIFT, in http://www.google.com/patents?vid=6711293